Practical Radiation Oncology (2014) **xx**, xxx–xxx

practical radiation oncology
pro
www.practicalradonc.org

Original Report

A contouring guide for head and neck cancers with perineural invasion

Huaising C. Ko BS [a], Vishal Gupta MD [a], Waleed F. Mourad MD [a, b, c], Kenneth S. Hu MD [a, b], Louis B. Harrison MD [a, b], Peter M. Som MD [d], Richard L. Bakst MD [a,*]

[a]*Department of Radiation Oncology, Icahn School of Medicine at Mount Sinai Hospital, New York, New York*
[b]*Department of Radiation Oncology, Mount Sinai at Beth Israel Medical Center, New York, New York*
[c]*Department of Radiation Oncology, Albert Einstein College of Medicine at Montefiore Medical Center, New York, New York*
[d]*Department of Radiology, Icahn School of Medicine at Mount Sinai Hospital, New York, New York*

Received 7 January 2014; revised 5 February 2014; accepted 5 February 2014

Abstract

Purpose: Perineural invasion (PNI) is a frequent pathological finding in head and neck cancers. When adjuvant radiation to cranial nerves at risk in head and neck cancers with PNI is considered, there is a need for consensus on which nerves are at risk and how to contour these nerves. This contouring guide attempts to address this need.

Methods and materials: Representative patient diagnostic computed tomographic (CT) scans with contrast of the neck were used to create example contours. The cranial nerves V_2, V_3, VII, and XII, and sample primary tumor sites were initially delineated using the Varian Eclipse planning system by 5 radiation oncologists. All of the images were then reviewed with a diagnostic radiologist to establish consensus for delineating the cranial nerves.

Results: We provided detailed contouring and planning guidelines on a CT atlas, with figures to help illustrate internerve connections, based on clinical experience, literature-based patterns of failure, and established anatomic connections between cranial nerves. Tumor bed, cranial nerve, and elective target volumes are depicted.

Conclusions: These planning guidelines and atlas provide anatomic, clinical, and technical recommendations for guiding radiation oncologists in the planning and delivery of intensity modulated radiation therapy for head and neck cancer with PNI.

Introduction

Perineural invasion (PNI) by cancers is a frequent pathologic finding and a significant cause of morbidity and mortality, conferring a poor prognosis.[1] PNI is a clinicopathologic entity generally defined as tumor cell invasion in, around, and through the nerves.[2] The term encompasses both "microscopic PNI," which is often only a histologic finding and "gross PNI," a clinical or radiologic observation, which is noted either by clinical symptoms such as paresthesia, paralysis, and numbness, or seen grossly in the operating room or

Conflicts of interest: None.

* Corresponding author. Department of Radiation Oncology, Icahn School of Medicine at Mount Sinai Hospital, 1184 5th Ave, New York, NY 10029.
E-mail address: Richard.Bakst@mountsinai.org (R.L. Bakst).

1879-8500/$ – see front matter
http://dx.doi.org/10.1016/j.prro.2014.02.001

diagnostic imaging. Radiographic evidence of PNI can be appreciated on a variety of imaging modalities, such as computed tomography (CT), magnetic resonance imaging, or positron emission tomography (Fig 1), which can play an important role in the detection of PNI.[3] This local extension of cancers cells along nerves is an ominous clinical event that is associated with increased local recurrence and worsened survival.[4-7] Currently, there are limited resources and guidelines for radiation oncologists to accurately target cranial nerves (CNs).[8-10] The existing Radiation Therapy Oncology Group cranial nerve atlas[9] only covers a limited set of the CNs potentially at risk for PNI. Our aim is to present a more comprehensive set of guidelines that will help radiation oncologists plan their contours for 5 common clinical case scenarios of head and neck cancer with PNI.

Methods and materials

CT scan selection

Representative patient diagnostic CT scans with contrast of the neck were used to create example contours. The axial CT slices taken at 3-mm intervals were imported into Varian Eclipse contouring software (Varian Medial Systems, Palo Alto, CA).

Delineation procedure

The CNs V_2, V_3, VII, and XII, and sample primary tumor sites were initially delineated by 5 radiation oncologists using the Eclipse planning system. All of the images were then reviewed with a diagnostic radiologist to establish

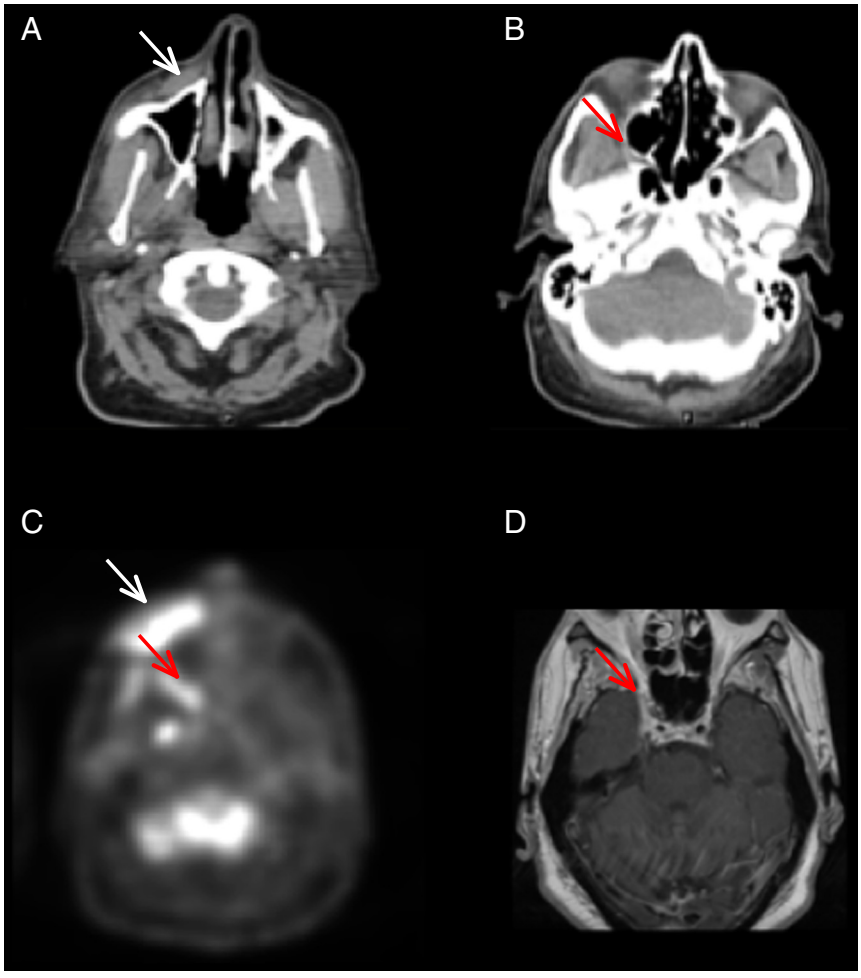

Figure 1 Radiographic example of perineural invasion. Axial computed tomographic (CT) image of squamous cell carcinoma of the malar cheek, with perineural invasion (PNI) of the right maxillary nerve (cranial nerve [CN] V_2), revealing the following: (A) Primary tumor (white arrow) and (B) thickening of the maxillary nerve, consistent with PNI by cancer (red arrow); (C) axial positron emission tomographic image reveals hypermetabolic lesions corresponding with the primary tumor (white arrow) and PNI in the maxillary nerve (red arrow); and (D) axial T1 postcontrast magnetic resonance image shows PNI in the maxillary nerve (red arrow).

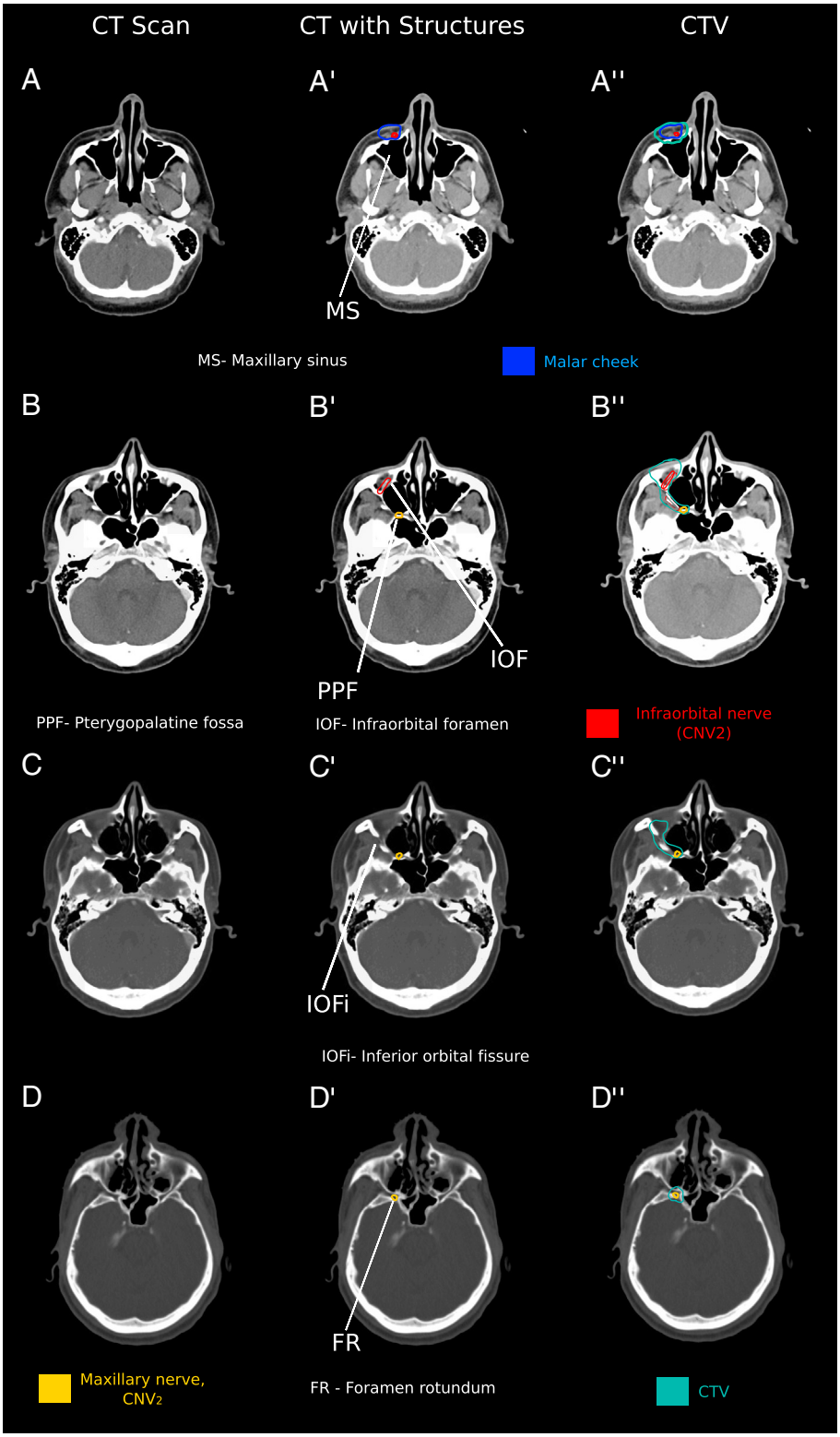

Figure 2 Axial computed tomographic (CT) slices of the malar cheek and related cranial nerves. The left column (A-D) depicts axial CT images of the area of interest, the middle column (A′-D′) depicts the nerves contoured on CT images, and the right (A″-D″) depicts these contours with a clinical target volume (CTV; shown in teal). The maxillary nerve (cranial nerve [CN] V_2) (shown in yellow) and its branch, the infraorbital nerve (shown in red), provide innervation to the malar cheek (shown in blue) and are at risk for harboring cancer in the setting of perineural invasion.

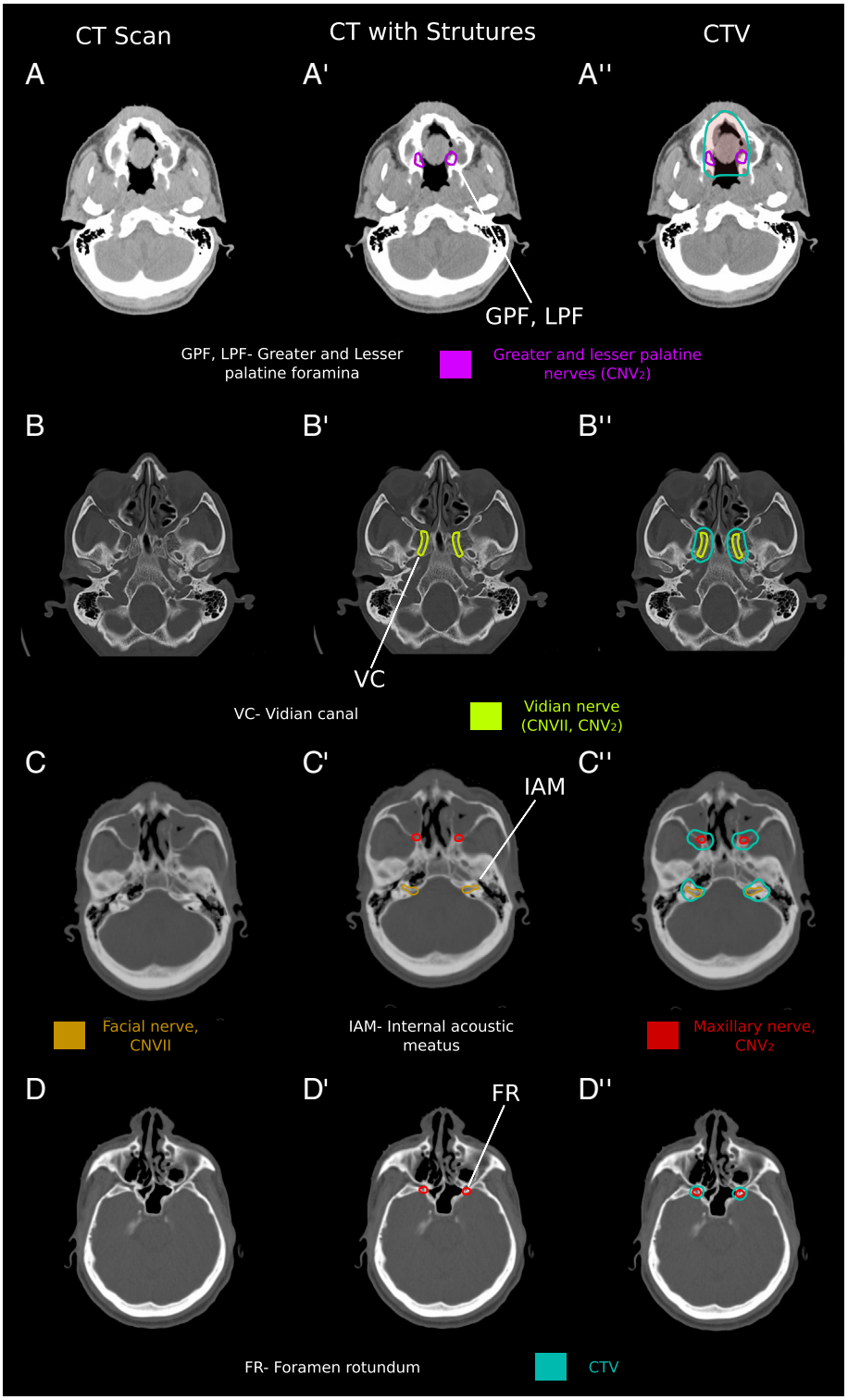

Figure 3 Axial computed tomographic (CT) slices of the hard palate and related cranial nerves. The left column (A-D) depicts axial CT images of the area of interest, the middle column (A′-D′) depicts the nerves contoured on CT images, and the right (A″-D″) depicts these contours with a clinical target volume (CTV; shown in teal). The maxillary nerve (cranial nerve [CN] V_2) (shown in red) and its branches, the greater and lesser palatine nerves (shown in purple), provide innervation to the hard palate. The facial nerve (CN VII) (shown in gold), can also be involved in cancers of the hard palate, through the vidian nerve (shown in yellow-green). The maxillary nerve, the facial nerve, and their aforementioned respective branches are at risk for harboring cancer in the setting of perineural invasion. (IAM, internal acoustic meatus.)

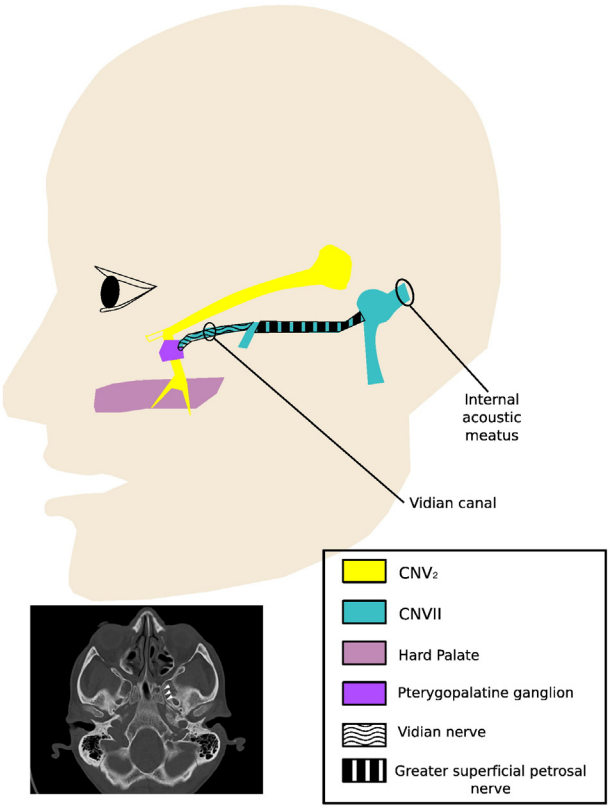

Figure 4 Schematic diagram of the internerve connections between cranial nerves [CN] V_2 and VII in the vicinity of the hard palate. Inset: A computed tomographic (CT) scan demonstrating the vidian canal (white arrowheads), where these 2 nerves communicate as the vidian nerve.

consensus for delineating the CNs. The CNs were contoured using soft tissue and bone CT windows setting to simulate a typical radiation planning environment.

Results

Malar cheek

The malar cheek region (Fig 2A-A″) generally refers to the skin and soft tissue superficial to the maxilla and the zygomatic bone. It is bordered superiorly by the inferior aspect of the orbital fossa, and inferiorly by oral cavity. From the malar cheek, the sensory innervation is supplied by the infraorbital nerve (a branch of CN V_2), which emerges from the infraorbital foramen in the maxilla (Fig 2B-B″). Tracking proximally, the infraorbital nerve travels along the infraorbital foramen until it leaves the orbit through the inferior orbital fissure (Fig 2C-C″), where it becomes the maxillary nerve. The maxillary nerve crosses the pterygopalatine fossa (Fig 2B) as it moves superiorly and proximally until its site of emergence from the base of skull at the foramen rotundum (Fig 2D-D″). In the case of incidental PNI, however, we do not routinely cover the course of the nerve to the foramen rotundum.

Hard palate

The hard palate is the bony plate occupying the superior aspect of the oral cavity (Fig 3A). As the hard palate is a midline structure, we consider bilateral coverage of the CNs in cases where both sides could be at risk for harboring tumor. Innervation to the hard palate is largely supplied by the greater and lesser palatine nerves, which are branches of the maxillary nerve (CN V_2). From the hard palate, the greater and lesser palatine nerves enter the bone through the greater and lesser palatine foramina (Fig 3A-A″), and travel superiorly through the greater palatine canal. At the proximal portion of the greater palatine canal, the nerve fibers join the pterygopalatine ganglion, whose preganglionic fibers arise from the maxillary nerve (CN V_2) and the vidian nerve (which arises from a branch of CN VII) (Fig 3B-B″). Tumors in the hard palate with perineural involvement may be at risk for spread to the facial nerve (Fig 3C; CN VII) via the vidian nerve and the greater superficial petrosal nerve (a branch of CN VII). The facial nerve inserts into the brain stem at the internal acoustic meatus (Fig 3C′). The maxillary nerve tracks proximally up into the foramen rotundum at the base of skull (Fig 3D), while the vidian nerve arises from the greater superficial petrosal nerve (a branch of CN VII).

We consider covering tumors of the hard palate with asymptomatic microscopic PNI to the maxillary nerve up to the foramen rotundum. Cases that involve gross or clinically evident PNI or are of adenoid cystic carcinoma (ACC) histologic subtype are additionally covered for the facial nerve from the vidian and greater superficial petrosal nerves up to the internal acoustic meatus (Fig 4).

Parotid gland

The parotid gland is a paired structure and the largest of the salivary glands, located inferior and anterior to the external acoustic meatus. Each parotid gland extends posteriorly to the mandibular ramus (Fig 5A-A″) and anterior to the mastoid process of the temporal bone. Tumors that involve the parotid gland risk the facial nerve (CN VII), which pierces through the gland. The CN VII enters the base of skull at the stylomastoid foramen and travels in the petrous portion of the temporal bone (Fig 5B-B″), ultimately entering the brain stem at the internal acoustic meatus (Fig 5D-D″).

The auriculotemporal nerve (a branch of CN V_3) provides innervation to the glandular tissue, placing CN V_3 at risk for PNI, therefore warranting coverage of the foramen ovale if appropriate (Fig 5C-C″). The auriculotemporal nerve communicates with CN VII near the medial posterior portion of the mandible.

For tumors of the parotid gland with microscopic PNI, we consider coverage to the facial nerve up to the stylomastoid foramen and the parapharyngeal space as the nerve tracks up to the skull base at the internal acoustic

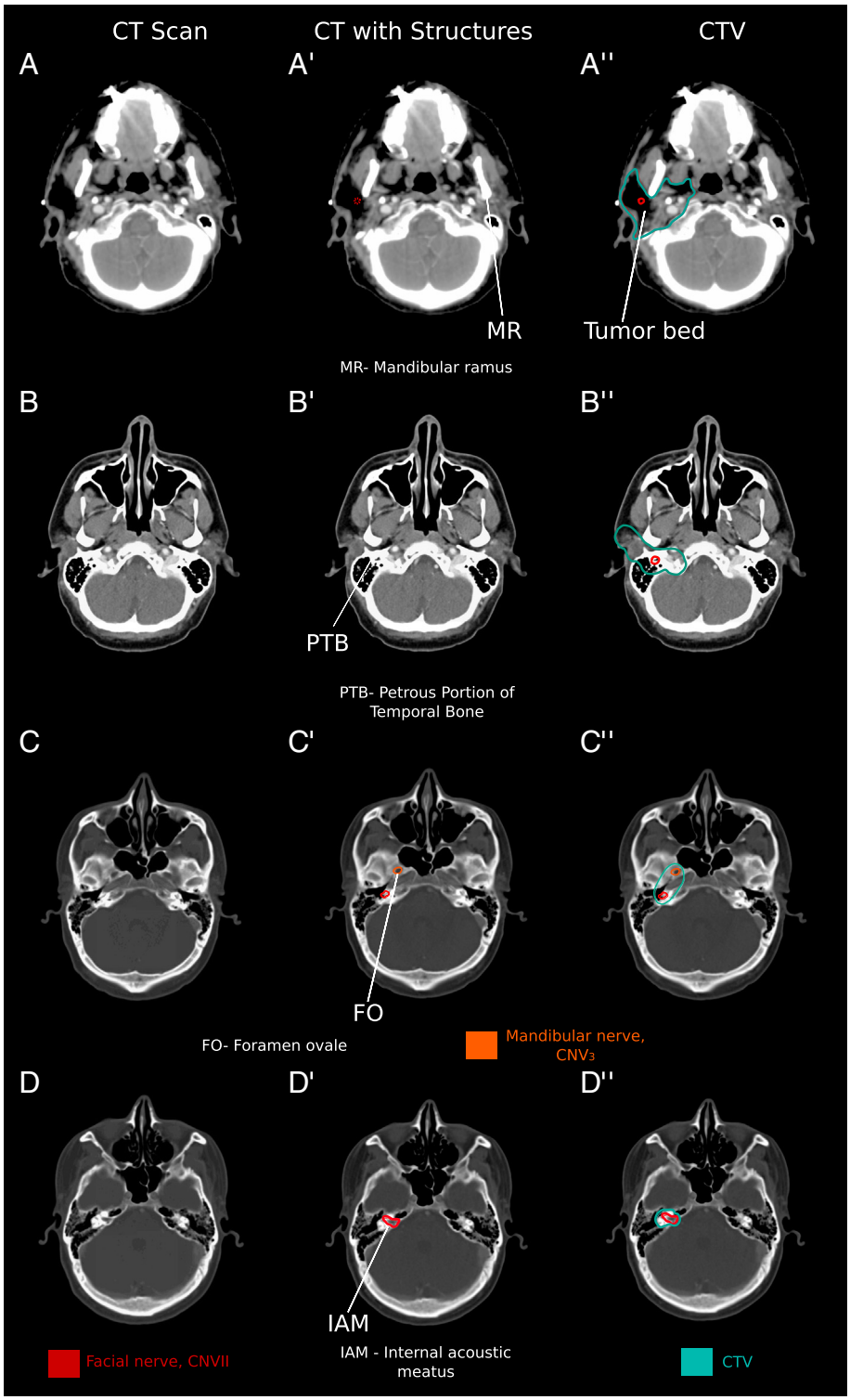

Figure 5 Axial computed tomographic (CT) slices of the parotid gland and related cranial nerves. The left column (A-D) depicts axial CT images of the area of interest, the middle column (A′-D′) depicts the nerves contoured on CT images, and the right (A″-D″) depicts these contours with a clinical target volumes (CTV; shown in teal). The facial nerve (cranial nerve [CN] VII) (shown in red), pierces the parotid gland tissue. The mandibular nerve (CN V_3) (shown in orange) can also be involved in cancers of the parotid gland via internerve connections. The mandibular nerve and the facial nerve are at risk for harboring cancer in the setting of perineural invasion.

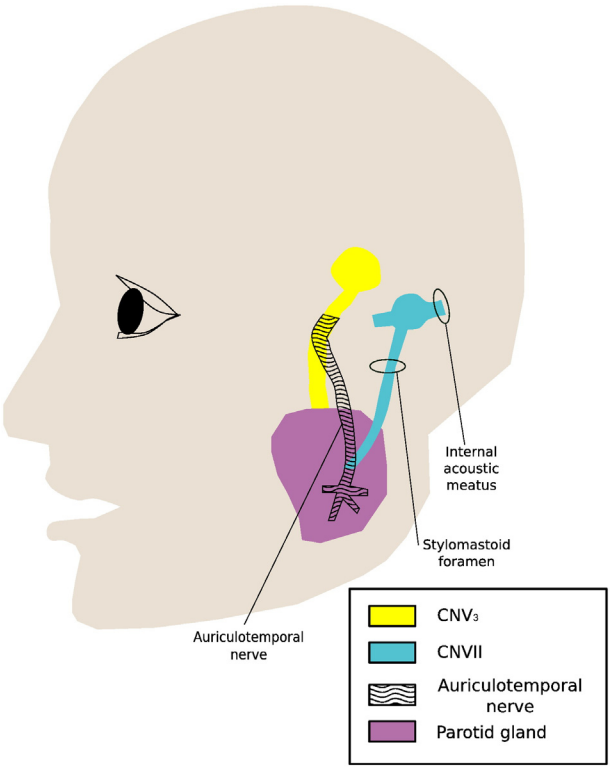

Figure 6 Schematic diagram of the internerve connections between cranial nerves (CNs) V_3 and VII in the vicinity of the parotid gland.

meatus. In those tumors that are of ACC histologic subtype, or feature gross PNI, we suggest additional coverage of the mandibular nerve from the auriculotemporal nerve up to the foramen ovale[11,12] (Fig 6).

Submandibular gland

The submandibular gland (SMG) is a paired structure, located in the submandibular fossa of the mandible (Fig 7A-A″). These glands receive their parasympathetic innervation from the branches of the lingual nerve (a branch of CN V_3) (Fig 7B-B″). The lingual nerve is 1 of 2 major branches that arise from the mandibular nerve (CN V_3), at the level of the mandibular foramen (Fig 7B). The mandibular nerve emerges from the base of skull at the foramen ovale (Fig 7D). The SMG also receives innervation from the facial nerve (CN VII) via the chorda tympani nerve, which eventually joins the lingual nerve (branch of CN V_3) (Fig 7D).

Tumors originating in the SMG with PNI pose a risk of involving the hypoglossal nerve (CN XII) by virtue of the nerve's proximity to the deep portion of the gland (Fig 7B). The hypoglossal nerve emerges from the base of skull at the hypoglossal canal (Fig 7C).

For tumors of the submandibular gland with microscopic PNI we consider coverage of the mandibular nerve up to the foramen ovale, and the hypoglossal nerve up to the hypoglossal canal only for tumors of the deep lobe of the submandibular gland with extraparenchymal extension. While there exists a true anatomic connection between the SMG and the facial nerve via the chorda tympani, failures of CN VII from these tumors are very rare.[13,14]

Lower lip

The lower lip (Fig 8A-D) is largely innervated by the mental nerve, which arises from the inferior alveolar nerve as emerges from the mental foramen of the mandible. The inferior alveolar nerve is a branch of the mandibular nerve (CN V_3) that travels inside the mandible after entering mandibular foramen (Fig 8B-B″). The mandibular nerve travels superiorly following the posterior border of the masticator space at the division of the lateral and medial pterygoid muscles (Fig 8C-C″). The mandibular nerve enters the skull at the foramen ovale (Fig 8D-D″).

Discussion

Cancers in which PNI is present represent a challenge for radiation oncologists. PNI, a prominent characteristic of head and neck cancers, has been reported in up to 80% of head and neck squamous cell carcinomas.[15] In particular, ACC, which accounts for 1%-2% of all head and neck cancers,[16] has a high propensity for PNI in up to 96% of cases.[3,17-19] In many cases, patients suffer from debilitating neuropathic pain, paralysis from motor nerve dysfunction, and numbness from sensory nerve dysfunction due to perineural cancer spread. The natural history of PNI allows the tumor to track proximally from the distal branches of the nerve toward the central nervous system, eventually leading to failures at the base of skull.[10,20] Tumor recurrences at the base of skull are a major concern, and are extremely difficult to salvage. Therefore, in ACC cases where the tumor has PNI, the involved nerves are often targeted up to their origin in the skull base.[21]

While the presence of PNI has been shown to be associated with poor clinical outcomes, the addition of adjuvant radiation remains controversial for patients with microscopic evidence of PNI alone at the time of surgery. The body of evidence for demonstrating benefit in local control for neurotrophic cancers comes only from retrospective studies.[16,21,22-24] These studies have demonstrated that postoperative radiation therapy can improve local control and reduce lethal base of skull recurrences.[21,23,24] However, they fail to come to a unified consensus on the pathologic indications for adjuvant radiation. Furthermore, there are some studies that demonstrate no added benefit for adjuvant radiation.[25] From the evidence discussed there is no clear path to best manage PNI, which is further complicated by the lack of prospective based studies.

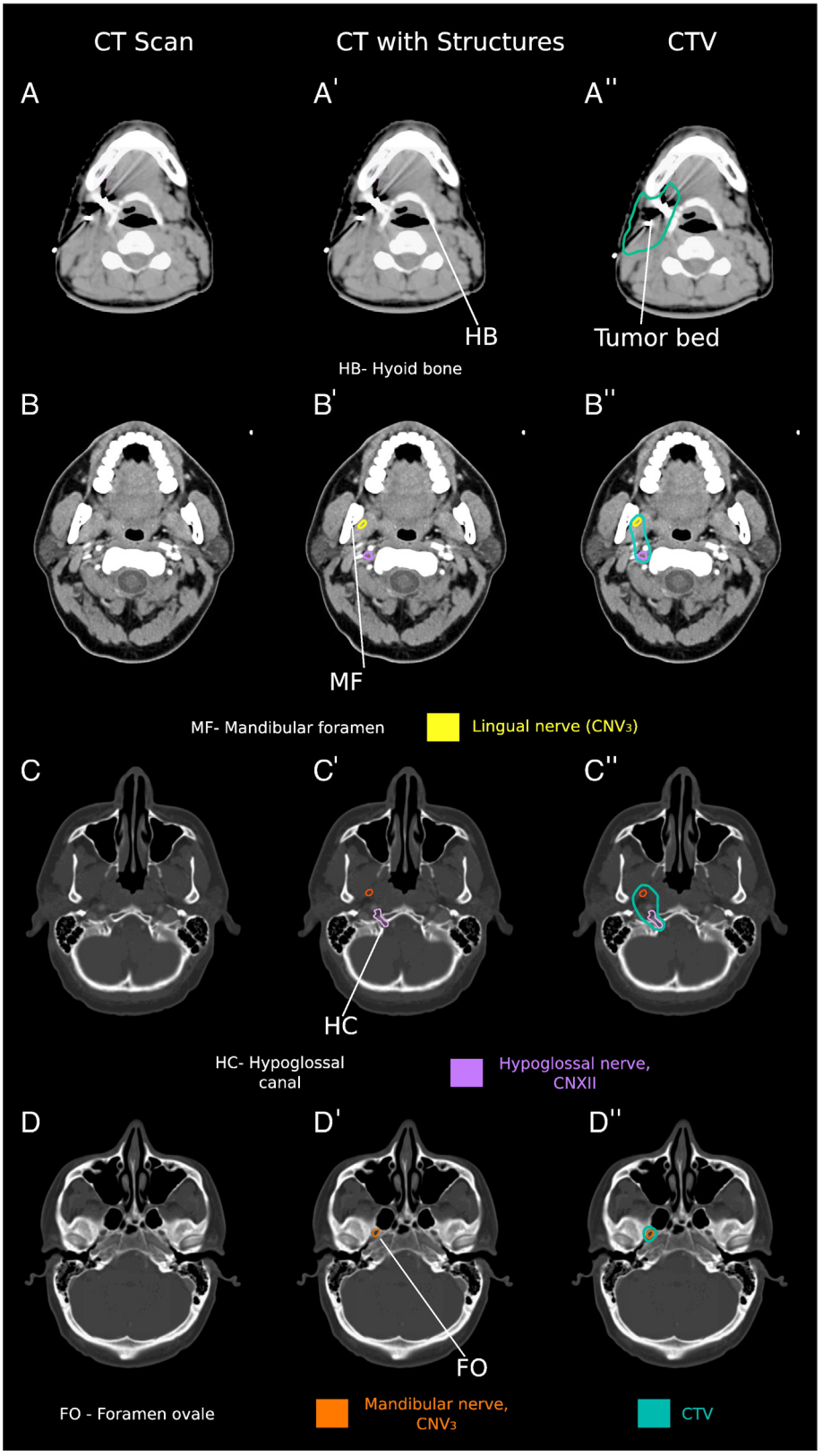

Figure 7 Axial computed tomographic (CT) slices of the submandibular gland and related cranial nerves (CN). The left column (A-D) depicts axial CT images of the area of interest, the middle column (A′-D′) depicts the nerves contoured on CT images, and the right (A″-D″) depicts these contours with a clinical target volume (CTV; shown in teal). The mandibular nerve (CN V_3) (shown in orange), and its branch, the lingual nerve (shown in yellow), provide innervation to the submandibular gland and are at risk for harboring cancer in the setting of perineural invasion. The hypoglossal nerve (CN XII) (shown in purple) can also be involved in cancers of the deep lobe of the submandibular gland.

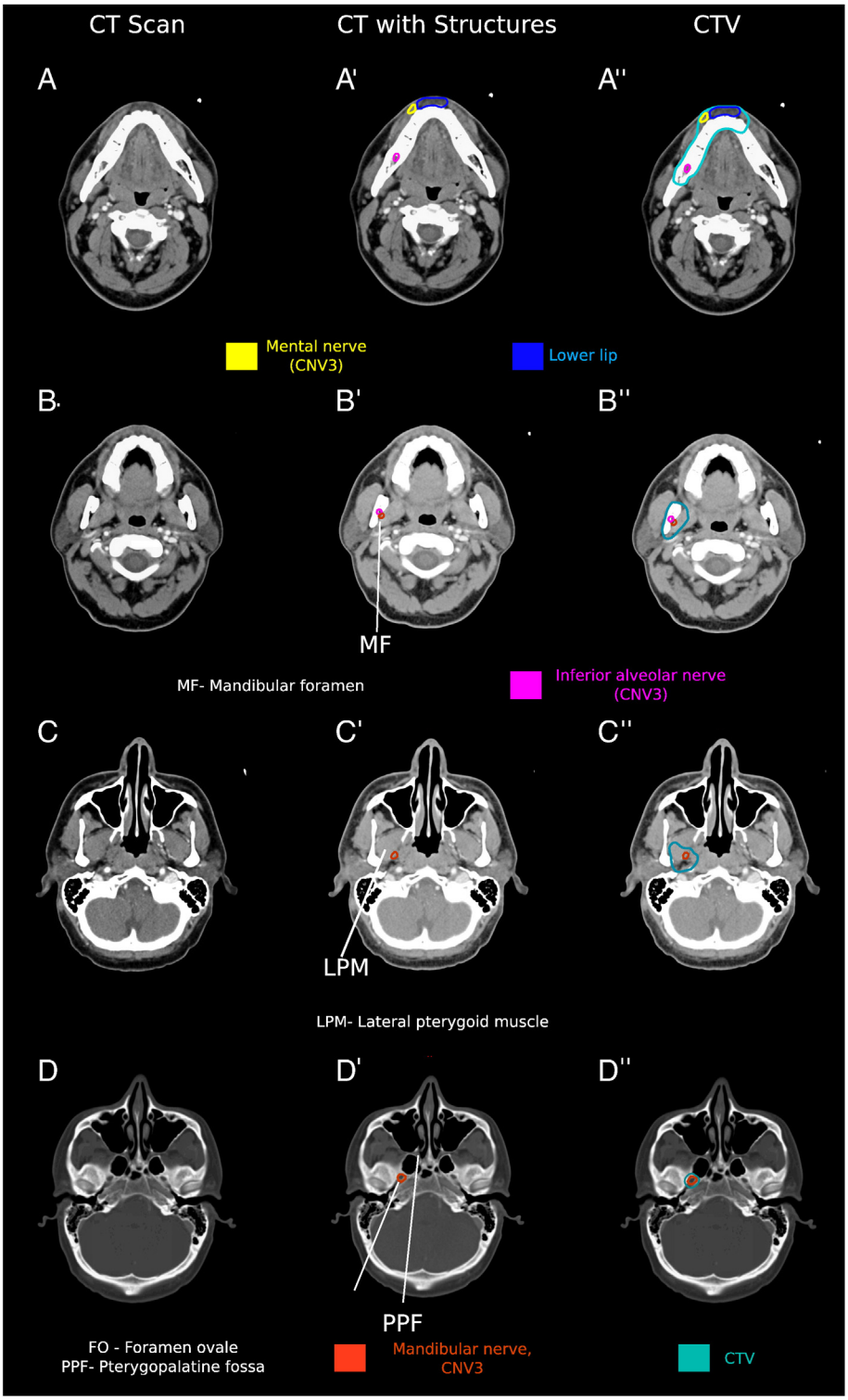

Figure 8 Axial computed tomographic (CT) slices of the lower lip and related cranial nerves. The left column (A-D) depicts axial CT images of the area of interest, the middle column (A′-D′) depicts the nerves contoured on CT images, and the right (A″-D″) depicts these contours with a clinical target volume (CTV; shown in teal). The mandibular nerve (cranial nerve [CN] V_3) (shown in orange), and its branches, the inferior alveolar nerve (shown in purple) and the mental nerve (shown in yellow), provide innervation to the lower lip (shown in blue), and are at risk for harboring cancer in the setting of perineural invasion.

While the general consensus is that adjuvant radiation in the context of cancer with PNI improves local control, further study is necessary to streamline and standardize adjuvant radiation in this setting.

The optimal radiation treatment volume with respect to tracing the CNs back to the skull is not well defined, and carries a significant risk of toxicity to adjacent critical structures. The difficulty of navigating the anatomy of the head and neck is further complicated by the intricacies and compact nature of the structures contained in this region. The importance of consistent and exact contours is further intensified by the level of precision that is afforded by modern intensity modulated radiation therapy (IMRT). In the era of IMRT, radiation oncologists are able to deliver 3-dimensional conformal radiation doses from CT scans with precision on the order of millimeters. The variation in outlining target volumes has been shown to be a major factor in the global uncertainty in radiation treatment planning.[26] Not only are these challenging cases but the intricate anatomy of the head and neck furthers the level of uncertainty. In this light, having a detailed and complete knowledge of the anatomic landscape is increasingly important.

In compiling this atlas, we have selected 5 common clinical cases that adequately represent the range and variety of head and neck cases with PNI: malar cheek, hard palate, parotid gland, submandibular gland, and lower lip. Cutaneous lesions of the malar cheek and lower lip are common sites of skin cancers that can feature PNI with rates in the range of 0.18%-10% in basal cell carcinomas and 2.5%-14% squamous cell carcinomas.[27,28] In fact, the cheek or midface location itself is a risk factor associated with the presence of PNI.[29] Cancers of the major and minor salivary glands, which include the parotid gland, submandibular gland, and the hard palate, can also involve PNI at rates of up to 43% of operable cancers at the time of surgery.[21] In light of these data, these 5 sites represent a range of possible clinical scenarios likely to be seen by a practicing radiation oncologist who encounters a head and neck cancer with PNI.

The contouring of relevant CNs is based on delineating anatomic areas with an approach that relies on clinical experience, literature-based patterns of failure, and established anatomic internerve connections in treating these cases. As such, this atlas serves as a suggested set of plans for managing head and neck cancers with PNI. While there exist a wide variation in treating these cases from institution to institution, here we provide a basic outline for suggested doses in different clinical scenarios, based on our experience. For cases of microscopic PNI with negative surgical margins on the nerve, our recommended dose is at least 54 Gy to the nerve course, while respecting all critical structure tolerances. For cases of gross PNI with negative margins on the nerve, our recommended dose increases to 60 Gy to the nerve course, respecting normal tissue tolerances. In the case of gross PNI with positive margins on the nerve, the recommended dose to the tumor bed is 66 Gy, with the remaining nerve course treated to 60 Gy, while respecting the brain stem's normal tolerance. The optimal doses in these cases are not well defined and warrant further study. Interestingly, there are preclinical data suggesting that lower doses may be effective in this setting[30]; however, it is not clear that lower doses are effective in human cancers.

Each clinical case can present a complexity that makes it difficult to determine which nerve structures are at risk and, among them, their relative levels of vulnerability. We hope to offer an evidence-based guide that can address these questions at a basic level (Table 1). For clinical scenarios with microscopic PNI of a named nerve, noted in the pathology report, we recommend a clinical target volume that extends at least 0.5 cm from the nerve. The nerves most at risk in microscopic PNI are those listed for their anatomic proximity to the primary lesion (Table 1, column 2). In the case of radiographic PNI, clinical evidence of cranial nerve involvement, or gross involvement of the nerve seen in the operating room, we would consider elective coverage of CNs at risk via internerve connections (Table 1, column 5). While these are general recommendation for most head and neck cancers of the skin and salivary glands, 1 particular histology (ACC) warrants a higher level of caution.[17-20] As ACC has a predilection for tracking proximally along nerve tissue toward the CNS, leading to failures at the base of skull, we would consider CNs connected via internerve connections to be at risk as well as the anatomically proximate nerves, even in cases of microscopic PNI. Below are 3 examples of how Table 1 can be used to guide clinical radiation treatment planning in cases of head and neck cancer with PNI.

Example 1

In the a case of carcinoma ex pleomorphic adenoma of the parotid with microscopic PNI (Table 1, row 3), we would consider coverage of the facial nerve (CN VII) to the base of skull, depending on the extent of the tumor in the deep lobe of the parotid. When tracking CN VII to the base of skull, we often dose paint to employ a lower dose at the site of the internal acoustic meatus to minimize ototoxicity. If this cancer were to feature gross PNI or be of ACC histologic subtype, then we additionally suggest the elective coverage of the mandibular nerve (CN V_3), based on a connection via the auriculotemporal nerve.

Example 2

In the case of high-grade mucoepidermoid carcinoma of the hard palate (Table 1, row 2), with microscopic PNI and no evidence of clinical PNI, we would consider coverage of CN V_2 to the base of skull at the foramen rotundum. Given no frank clinical or radiographic

Table 1 Cranial nerves at risk with respect to location of head and neck malignancy

Site of primary	Cranial nerves at risk via anatomic proximity to primary lesion	Origin at base of skull	Relevant branches	Elective coverage of cranial nerves at risk via internerve connections	Documented patterns of failure (Reference)
Malar cheek	V_2	V_2: foramen rotundum	Infraorbital nerve	—	[7,9]
Hard palate	V_2	V_2: foramen rotundum	Greater and lesser palatine nerves	VII via greater superficial petrosal nerve and vidian nerve	[9,18]
[18]Parotid gland	VII	VII: stylomastoid foramen, internal acoustic meatus	—	V_3 via auriculotemporal nerve	[7,9,12,19]
Submandibular gland	V_3 XII [a]	V_3: foramen ovale XII [a]: hypoglossal canal	Lingual nerve	—	[19]
Lower lip	V_3	V_3: foramen ovale	Mental nerve	—	[9,19]

[a] For deep lobe tumors of the submandibular gland with extraparenchymal extension only.

evidence of PNI, we would not cover the greater superficial petrosal nerve or the vidian nerve.

Example 3

In the case of a large T3 lesion of ACC in the deep portion of the submandibular gland, with microscopic PNI (Table 1, row 4), coverage of CNs V_3 and XII would be considered on the basis of anatomic proximity to the primary tumor.

Conclusions

We hope to set forth an accessible resource for clinicians managing head and neck cancers with PNI to help identify which CNs are relevant for a particular case, as well as provide anatomic landmarks to properly identify the course to the base of skull. It is our goal to increase consistency, precision, and accuracy for clinicians who treat these cases. While the radiation doses based on clinical scenario represent recommendations based on typical cases treated at our institutions, we leave the final decisions regarding treatment parameters to the discretion of the clinician until further study provides clearer guidelines.

References

1. Chinn SB, Spector ME, Bellile EL, et al. Impact of perineural invasion in the pathologically N0 neck in oral cavity squamous cell carcinoma. *Otolaryngol Head Neck Surg.* 2013;149:893-899.
2. Batsakis JG. Nerves and neurotropic carcinomas. *Ann Otol Rhinol Laryngol.* 1985;94(4 Pt 1):426-427.
3. Stambuk HE. Perineural tumor spread involving the central skull base region. *Semin Ultrasound CT MR.* 2013;34:445-458.
4. Liebig C, Ayala G, Wilks JA, Berger DH, Albo D. Perineural invasion in cancer: A review of the literature. *Cancer.* 2009;115:3379-3391.
5. Fagan JJ, Collins B, Barnes L, D'Amico F, Myers EN, Johnson JT. Perineural invasion in squamous cell carcinoma of the head and neck. *Arch Otolaryngol Head Neck Surg.* 1998;124:637-640.
6. Goepfert H, Dichtel WJ, Medina JE, Lindberg RD, Luna MD. Perineural invasion in squamous cell skin carcinoma of the head and neck. *Am J Surg.* 1984;148:542-547.
7. Soo KC, Carter RL, O'Brien CJ, Barr L, Bliss JM, Shaw HJ. Prognostic implications of perineural spread in squamous carcinomas of the head and neck. *Laryngoscope.* 1986;96:1145-1148.
8. Gluck I, Ibrahim M, Popovtzer A, et al. Skin cancer of the head and neck with perineural invasion: Defining the clinical target volumes based on the pattern of failure. *Int J Radiat Oncol Biol Phys.* 2009;74:38-46.
9. Mourad WF, Hu KS, Harrison LB. Cranial nerves IX–XII contouring atlas for head and neck cancer: Cranial nerves atlas. Available at http://www.rtog.org/CoreLab/ContouringAtlases/HNAtlases.aspx-3/8/2013. Accessed April 20, 2013.
10. Mourad WF, Young BM, Young R, et al. Clinical validation and applications for CT-based atlas for contouring the lower cranial nerves for head and neck cancer radiation therapy. *Oral Oncol.* 2013;49:956-963.
11. Ginsberg LE. MR imaging of perineural tumor spread. *Neuroimaging Clin N Am.* 2004;14:663-677.
12. Chan M, Dmytriw AA, Bartlett E, et al. Imaging of auriculotemporal nerve perineural spread. *Ecancermedicalscience.* 2013;7:374.
13. Bagatin M, Zeljko O, Mohammed AM. Perineural invasion by carcinoma of the lower lip. *J Craniomaxillofac Surg.* 1995;23:155-159.
14. Ginsberg LE. Imaging of perineural tumor spread in head and neck cancer. *Semin Ultrasound CT MR.* 1999;20:175-186.
15. Kurtz KA, Hoffman HT, Zimmerman MB, Robinson RA. Perineural and vascular invasion in oral cavity squamous carcinoma: Increased incidence on re-review of slides and by using immunohistochemical enhancement. *Arch Pathol Lab Med.* 2005;129:354-359.
16. Kim KH, Sung MW, Chung PS, Rhee CS, Park CI, Kim WH. Adenoid cystic carcinoma of the head and neck. *Arch Otolaryngol Head Neck Surg.* 1994;120:721-726.
17. Garden AS, Weber RS, Morrison WH, Ang KK, Peters LJ. The influence of positive margins and nerve invasion in adenoid cystic carcinoma of the head and neck treated with surgery and radiation. *Int J Radiat Oncol Biol Phys.* 1995;32:619-626.
18. Barrett AW, Speight PM. Perineural invasion in adenoid cystic carcinoma of the salivary glands: A valid prognostic indicator? *Oral Oncol.* 2009;45:936-940.
19. Dodd GD, Jing BS. Radiographic findings in adenoid cystic carcinoma of the head and neck. *Ann Otol Rhinol Laryngol.* 1972;81:591-598.
20. Laine FJ, Braun IF, Jensen ME, Nadel L, Som PM. Perineural tumor extension through the foramen ovale: Evaluation with MR imaging. *Radiology.* 1990;174:65-71.

21. Chen AM, Garcia J, Granchi P, Bucci MK, Lee NY. Base of skull recurrences after treatment of salivary gland cancer with perineural invasion reduced by postoperative radiotherapy. *Clin Otolaryngol.* 2009;34:539-545.
22. Garden AS, Weber RS, Ang KK, Morrison WH, Matre J, Peters LJ. Postoperative radiation therapy for malignant tumors of minor salivary glands. Outcome and patterns of failure. *Cancer.* 1994;73: 2563-2569.
23. Garden AS. el-Naggar AK, Morrison WH, Callender DL, Ang KK, Peters LJ. Postoperative radiotherapy for malignant tumors of the parotid gland. *Int J Radiat Oncol Biol Phys.* 1997;37:79-85.
24. Gomez DR, Hoppe BS, Wolden SL, et al. Outcomes and prognostic variables in adenoid cystic carcinoma of the head and neck: A recent experience. *Int J Radiat Oncol Biol Phys.* 2008;70:1365-1372.
25. Kokemueller H, Eckardt A, Brachvogel P, Hausamen JE. Adenoid cystic carcinoma of the head and neck–a 20 years experience. *Int J Oral Maxillofac Surg.* 2004;33:25-31.
26. Fuller CD, Nijkamp J, Duppen JC, et al. Prospective randomized double-blind pilot study of site-specific consensus atlas implementation for rectal cancer target volume delineation in the cooperative group setting. *Int J Radiat Oncol Biol Phys.* 2011;79:481-489.
27. Leibovitch I, Huilgol SC, Selva D, Hill D, Richards S, Paver R. Cutaneous squamous cell carcinoma treated with Mohs micrographic surgery in Australia II. Perineural invasion. *J Am Acad Dermatol.* 2005;53:261-266.
28. Ballantyne AJ. Perineural invasion by SCC. *J Dermatol Surg Oncol.* 1984;10:502-504.
29. Mendenhall WM, Amdur RJ, Hinerman RW, et al. Skin cancer of the head and neck with perineural invasion. *Am J Clin Oncol.* 2007;30: 93-96.
30. Bakst RL, Lee N, He S, et al. Radiation impairs perineural invasion by modulating the nerve microenvironment. *PLoS One.* 2012;7: e39925.